

MEMS Engineer Forum 2014

PL8

: MEMS R&D Activities in SAIT

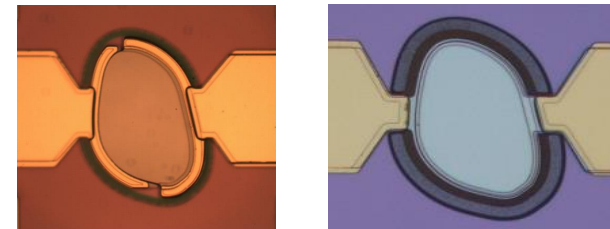


Hyungjae Shin

Samsung Advanced Institute of Technology

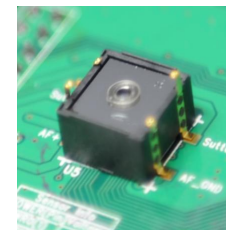
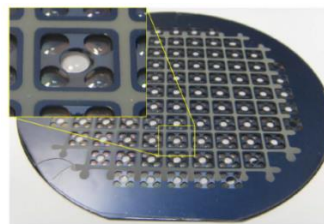
RF MEMS

- The first contribution from MEMS technology to mobile communication would be the passive elements and filters for band selection. Optimization of MEMS resonator for RF filter is presented.



Optical MEMS

- Miniaturization is one of MEMS' many advantages. Realization of many functional components of camera system and integration of these components to complete MEMS camera module is disclosed.



Acoustic MEMS

- Ultrasound is most harmless way to probe one's body, however, current technology's limited performance makes it difficult to widely accepted. The whole development process for new ultrasonic transducer is discussed.



RF MEMS

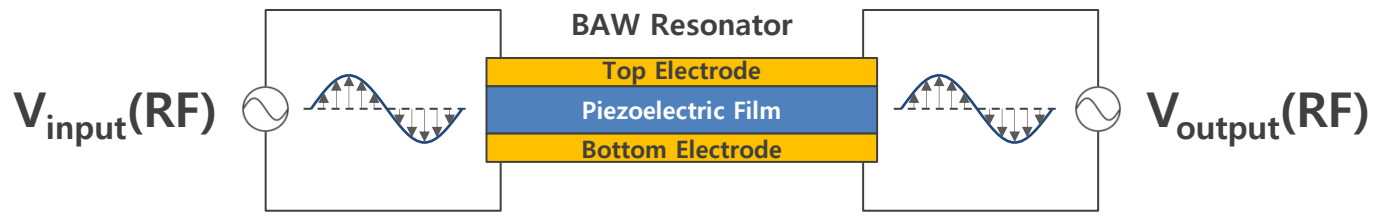
Performance Optimization of BAW Resonator



Contributors :

Hosoo Park, Insang Song, Moon-Chul Lee,
Jea-Shik Shin, Sang Uk Son, Chul-Soo Kim,
Jing Cui, Ai Yujie, Duck-Hwan Kim

Bulk Acoustic Wave (BAW) Resonator



Electric Energy

High speed microwave
 $\lambda \sim 15\text{cm}$ @2GHz in Air

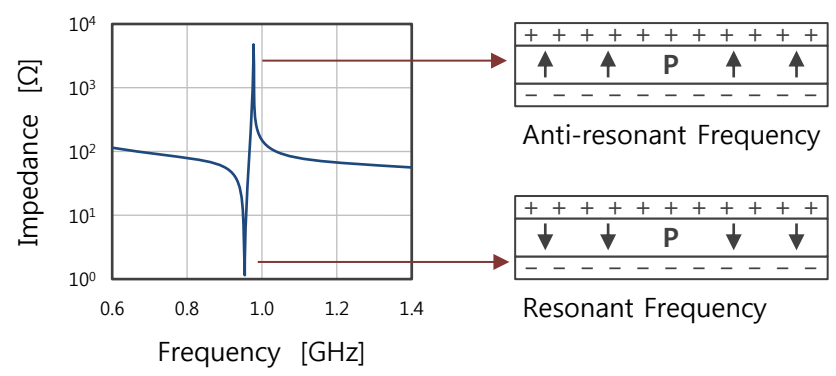
Acoustic Energy

Low speed acoustic wave
 $\lambda \sim 5\mu\text{m}$ in Solid AlN

Electric Energy

High speed microwave
 $\lambda \sim 15\text{cm}$ @2GHz in Air

Characteristics of BAW Resonator



Characteristics	SAW	BAW
Acoustic Q factor	< 200	> 1,000
Thermal Stability	-50ppm/°C	~±30ppm/°C
Power Handling	< 1W	> 1W
Process Materials	LiTaO ₃	Si, GaAs

● Performance Parameters of BAW Resonator

- Resonant & Anti-resonant frequencies
- Electro-mechanical coupling constant (kt^2) influences on the filter bandwidth
- Q-factor controls the roll-off
- Acoustic & electric loss impact on insertion loss of the filter

$$f = \frac{V_a}{2d}, \quad V_a = \sqrt{\frac{c}{\rho}}$$

$$kt^2 = \left(\frac{\pi f_r}{2 f_a} \right) / \tan\left(\frac{\pi f_r}{2 f_a} \right)$$

$$Q = \frac{f_r}{2} \left| \frac{\partial \phi_r}{\partial f} \right|_{\max}$$

$$= \frac{f_r}{2} \frac{Z_{ph}(r) - Z_{ph}(r-1)}{f_r - f_{r-1}}$$

f : frequency

V_a : acoustic velocity

d : thickness

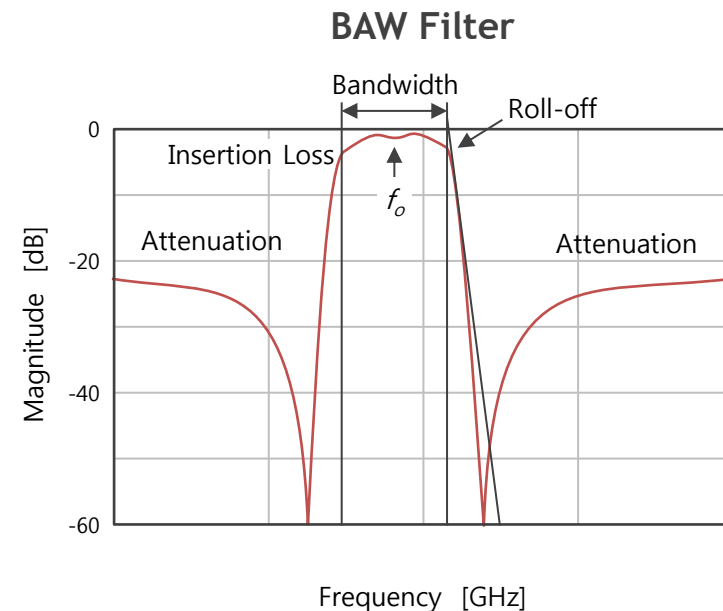
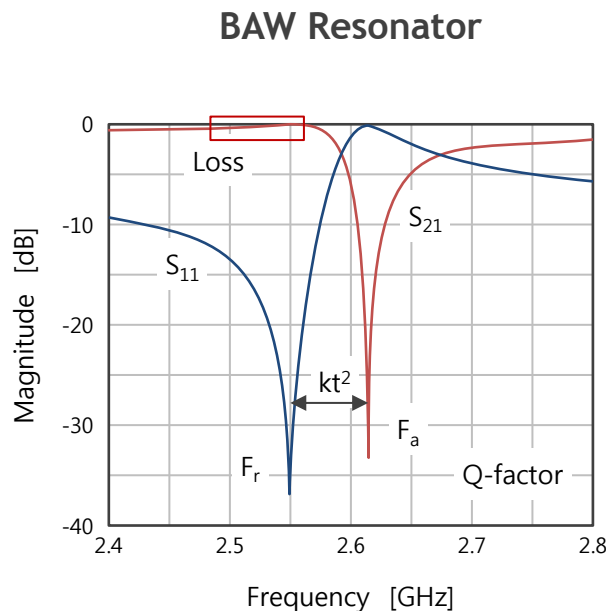
c : stiffness

ρ : density

f_{r-1} : previous frequency of f_r

$Z_{ph}(r)$: phase of f_r

$Z_{ph}(r-1)$: previous phase of f_r



● Various Standards of Wireless Communication

- Frequency resource is limited and becoming more expensive
- Band gap is getting narrower
- Low loss filter profile as well as high-Q resonator are required

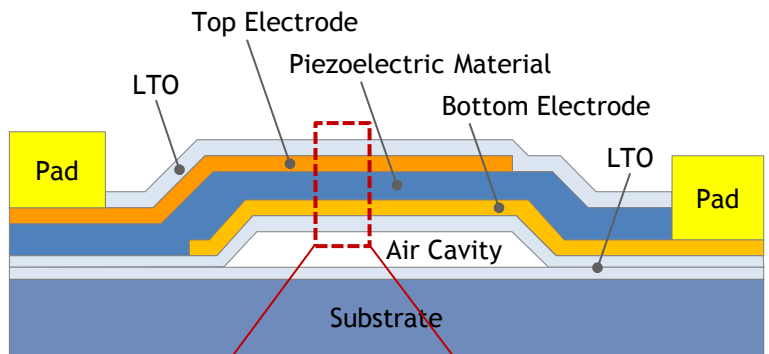
3GPP Name	3GPP2 Name	Common Name	Frequency [MHz]		$\Delta f/f_0$ [%]	Technology	Regional Area
			Up Link	Down Link			
Band-I	Band-6	IMT	1920-1980	2110-2170	6.4	SAW, BAW	Europe, Asia, Japan, Australia, New Zealand
Band-II	Band-1	PCS	1850-1910	1930-1990	1.0	BAW	North America
Band-III	Band-8	DCS	1710-1785	1805-1880	1.1	BAW	Europe, Asia
Band-IV	Band-15	AWS	1710-1755	2110-2155	18.4	SAW, BAW	USA, Canada(future)
Band-V	Band-0	CLR	824-849	869-894	2.3	SAW, BAW	North America, Australia, New Zealand, Philippine, Korea
Band-VI	Band-13	J-850MHz	830-840	875-885			
Band-VII	Band-16	IMT-E	2500-2570	2620-2690	1.9	BAW	Europe(future)
Band-VIII	Band-9	GSM	880-915	925-960	1.1	SAW, BAW	Europe, Asia, Australia, New Zealand
Band-IX		1.7MHz	1750-1785	1845-1880			
Band-X		E-AWS	1710-1770	2110-2170			
Band-XI		1.5MHz	1427-1452	1475-1500			
Band-XII	Band-19	L-700MHz	698-716	728-746	1.7	SAW, BAW	USA
Band-XIII	Band-7	U-700MHz	776-787	746-757			
Band-XIV	Band-18	U-700MHz	788-793	758-763			
	Band-14	PCS+G	1850-1915	1930-1995	0.8	BAW	USA

● Schematics of BAW Resonator

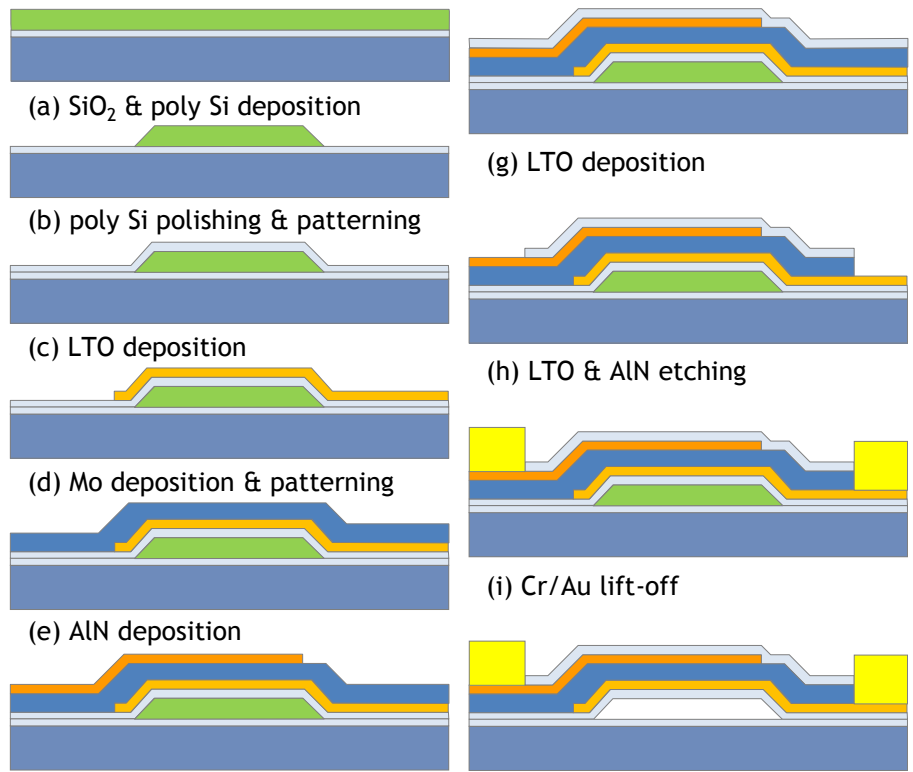
- Piezoelectric material (AlN) sandwiched between top & bottom electrodes

● Fabrication Process

- 13 masked Si process based on the surface micromachining technique



LTO=2,000Å
Ru=2,400Å
AlN=7,000Å
Mo=2,600Å
LTO=500Å



(f) Ru deposition & patterning

(j) Poly Si release

- **Electrical Loss**

- Electrode resistance, bonding pads & wiring

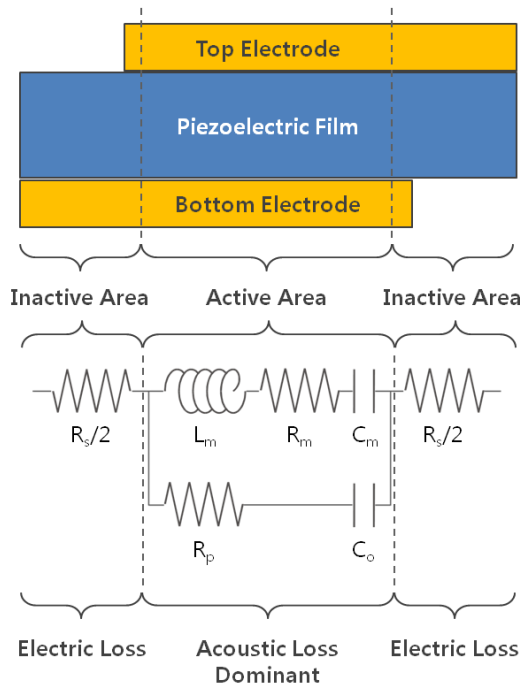
- **Mechanical Loss**

- Internal friction & damping during vibration

- **Acoustic Loss**

- Longitudinal leakage reduced by air cavity or alternating Bragg reflectors
- Lateral leakage by standing wave to be discussed

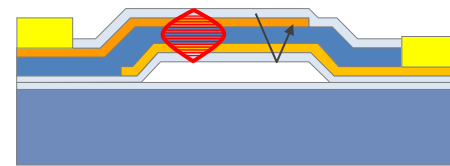
BAW Resonator & mBVD Model



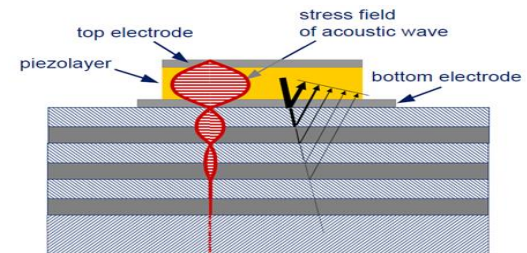
C_o : Static capacitance
 R_p : Material loss resistance
 L_m : Motional inductance
 R_m : Mechanical loss resistance
 C_m : Motional capacitance
 $R_s/2$: Electrode resistance

Longitudinal Acoustic Wave Leakage

Air Cavity Reflector



Alternating Bragg Reflectors



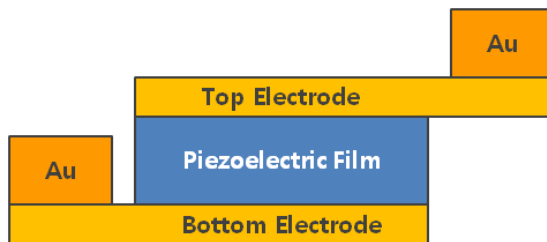
● Adoption of Au

- Au, in addition to Ru of top electrode and Mo of bottom electrode, to reduce the electrode resistance without compromise acoustic performance
- Adding Au band at the perimeter of the cavity to reduce the loss

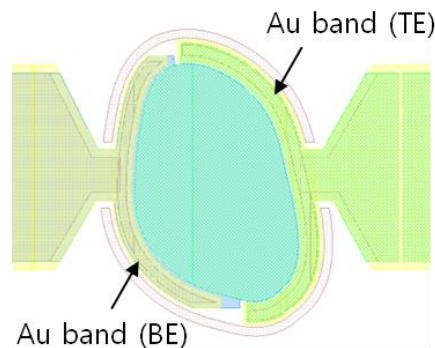
● Air-edge Reflector

- Creates lateral air interface to suppress the acoustic wave leakage

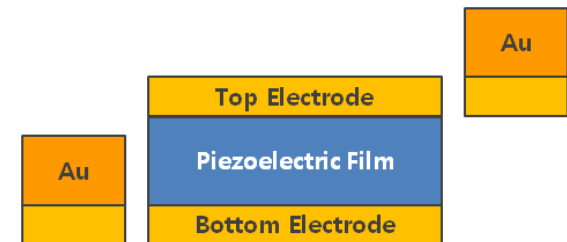
Au Electrode



Au Band



Air-edge Reflector



Sheet resistances

Au : 0.01 Ω /sq
Ru : 0.30 Ω /sq
Mo : 0.50 Ω /sq

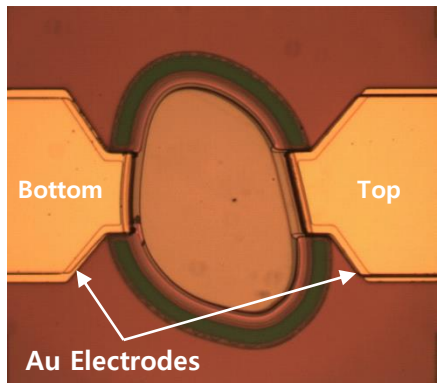
Acoustic Impedance

Air, ~ 404 , is 5 order higher than other materials, therefore, makes it a perfect reflector

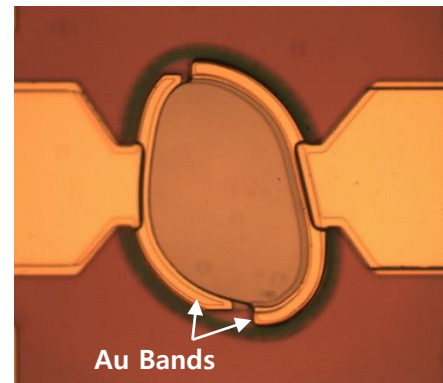
Expected Benefits of Au Band

- Improvement of insertion loss and Q-factor at the resonant frequency

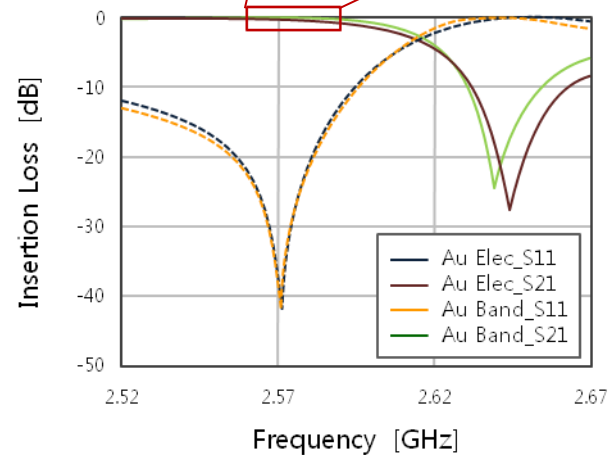
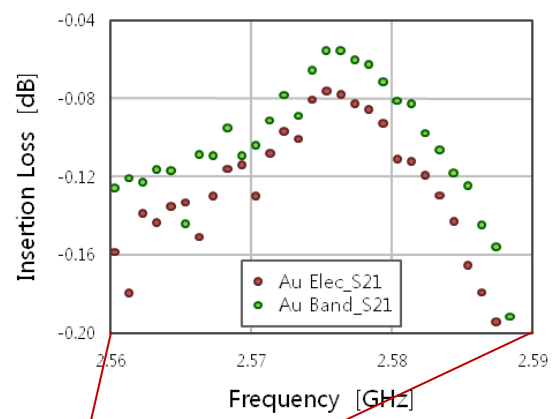
Added Au Electrode



Added Au Band



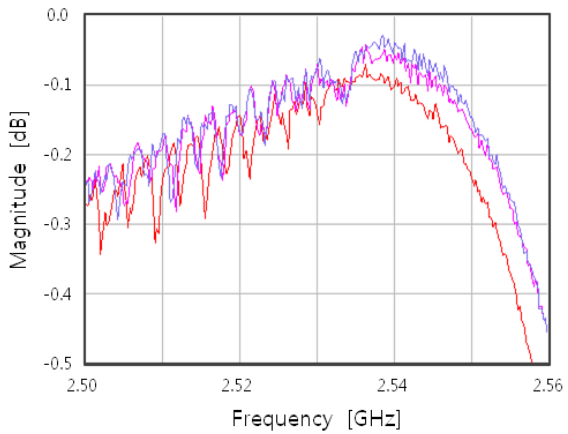
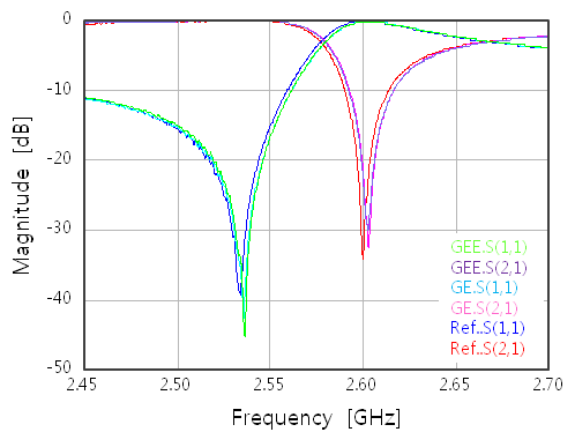
Simulated Results



	Resonant Freq.	Anti-resonant Freq.
with Au Electrodes		
with Au Perimeter Bands		

● Performance Improvements

- Insertion loss reduced from -0.05dB down to -0.03dB
- Q-factor enhanced by 37%
- Electrode resistance reduced down to 75.7%
- Degraded amount of kt^2 is sustained minimum



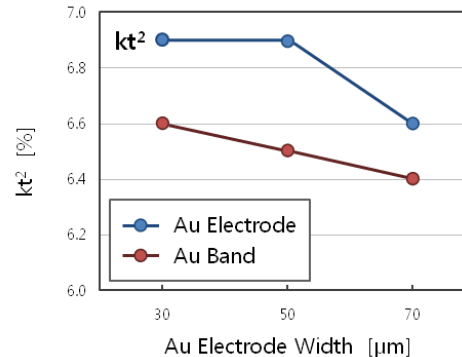
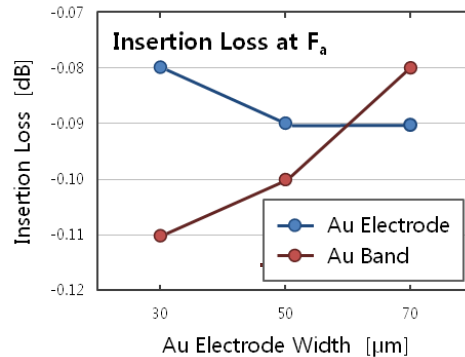
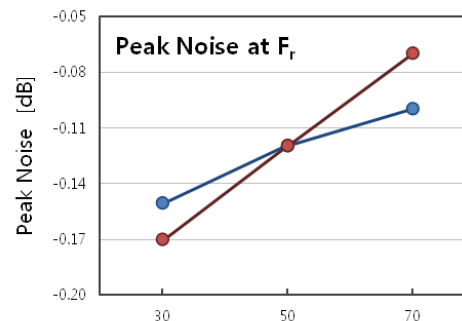
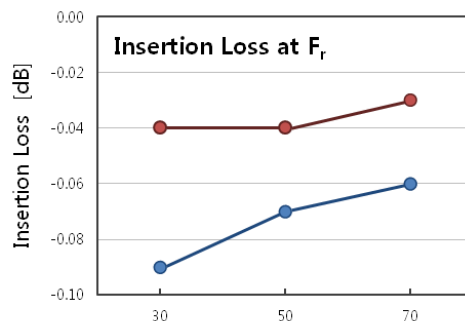
	Au electrode	Au band
Insertion Loss @ F_r (dB)	-0.05	-0.03
Insertion Loss @ F_a (dB)	-0.09	-0.08
Peak Noise @ F_r (dB)	-0.10	-0.07
kt^2 (%)	6.62	6.50
Q-factor @ F_r	995	1,360
$R_s/2$ (Ω)	1.07	0.81

Width Optimization of Au Electrode

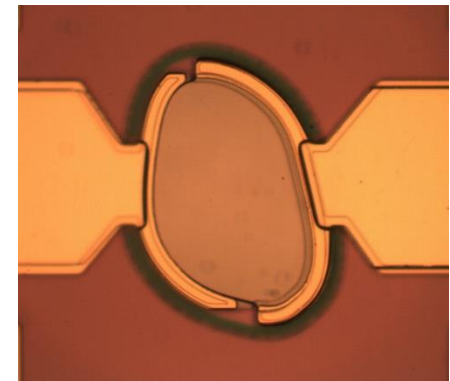
- Insertion loss reduced from -0.09dB to -0.06dB
- Peak noise suppressed from -0.15dB to -0.10dB
- kt^2 degraded 4.3%

Width Optimization of Au Band

- Insertion loss reduced from -0.06dB to -0.03dB
- Peak noise suppressed from -0.10dB to -0.07dB
- kt^2 degraded 3.0%



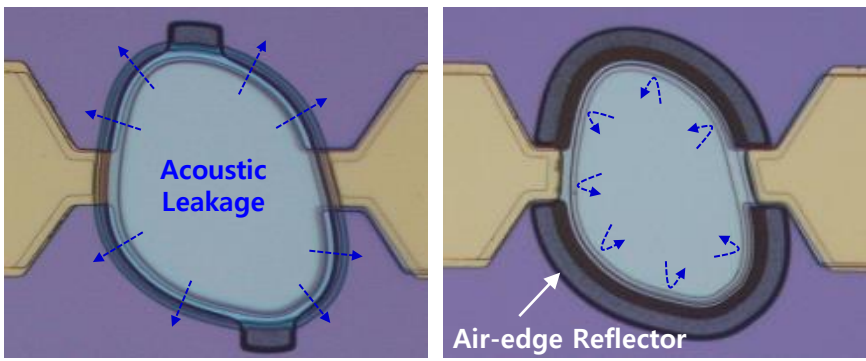
$$kt^2 = \frac{A}{\tan(A)} \times 100(\%) , \text{ where } A = \frac{\pi}{2} \times \frac{F_r}{F_a}$$



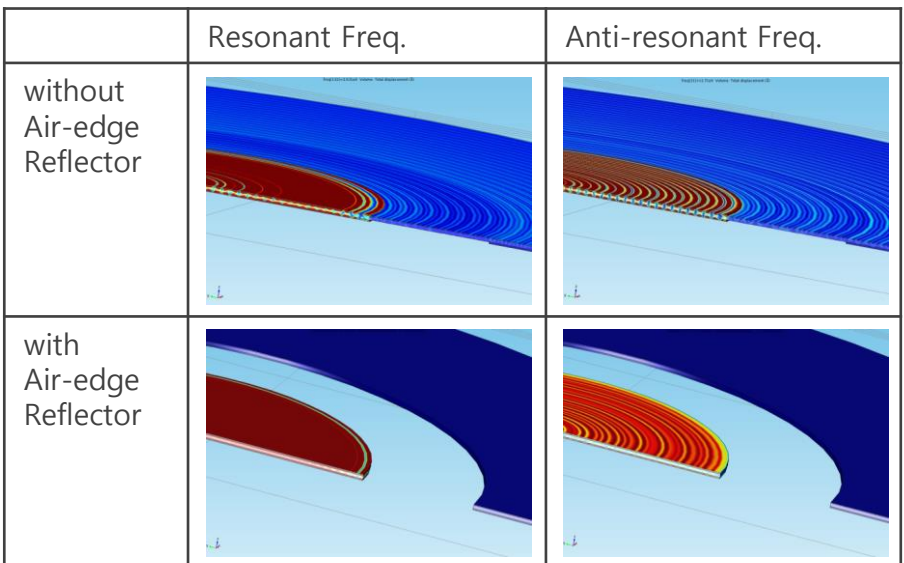
- Expected Benefits of Air-edge Reflector
 - Improvement of insertion loss, Q-factor and kt^2

Without Air-edge

With Air-edge



Simulated Results



$$R = \left(\frac{Z_2 - Z_1}{Z_2 + Z_1} \right)^2$$

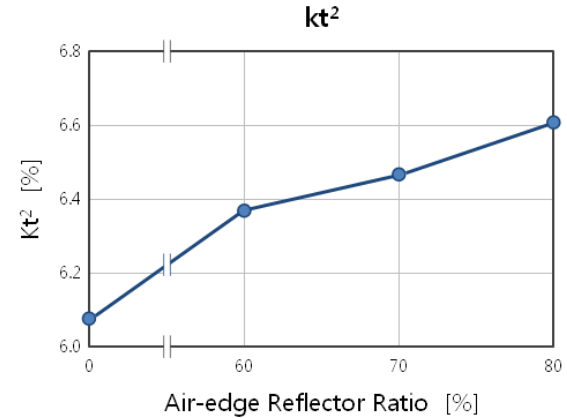
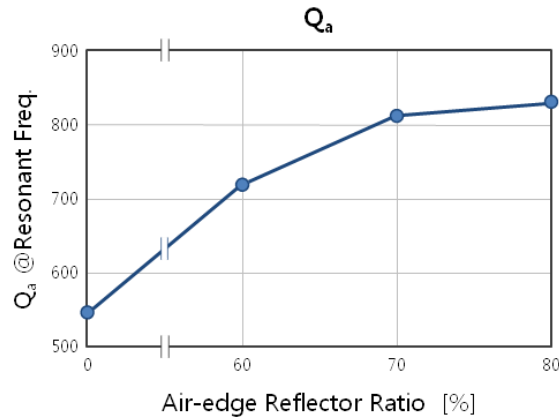
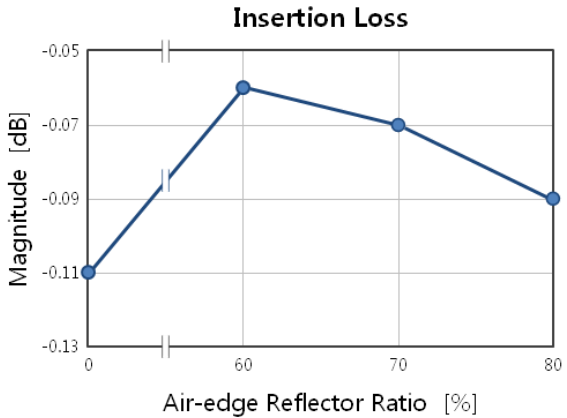
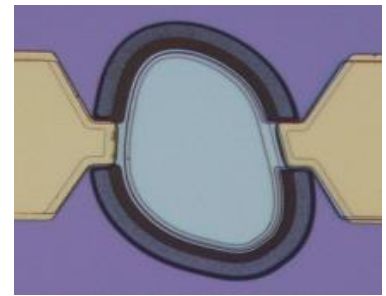
$$Z_a = \rho \times v_a = \sqrt{\rho \times C}$$

Material	Density [kg/m ³]	Stiffness [GPa]	Acoustic Velocity [m/sec]	Acoustic impedance [$\times 10^6$ kg/m ² s]
Ru	12,400	432	5,902	73.2
AlN	3,200	369	10,738	34.4
Mo	10,300	329	5,652	58.2
Si ₃ N ₄	2,850	309	10,413	29.7
SiO ₂	2,200	80	6,030	13.3
Air	1.2	1.4	33,912	0.04

Parameters		w/o Air-edge	w/ Air-edge
F _a	(MHz)	2,710	2,715
F _r	(MHz)	2,631	2,631
F _a - F _r	(MHz)	79	84
Insertion Loss	(dB)	0.12	0.11
S21 Pole	(dB)	29	34
kt ²	(%)	7.0	7.4
Q _a		910	1,070
Q _r		784	860

Performance Improvements

- Insertion loss reduced from -0.12dB down to -0.06dB
- Q_a -factor enhanced by 47%
- kt^2 improved 0.5%
- Needs to be optimized with electrode width for Insertion loss



● Au Electrode

- Application of Au in the inactive resonant area of electrodes lowered the electric resistance without sacrificing the acoustic losses

● Au Band

- Enlarged Au band at the perimeter of resonators improved performances

● Air-edge Reflector

- Lateral air interface was created to suppress the acoustic wave leakage

Optical MEMS

- . Liquid Lens for Auto Focus
- . Micromechanical Shutter
- . MEMS Camera
- . Tunable Optics for Medical Imaging



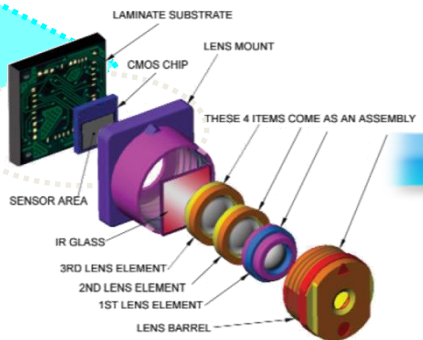
Contributors :

Woonbae Kim, Che-Heung Kim, JongOh Kwon
Kyu-Dong Jung, JeongYub Lee, Eunsung Lee
Seungwan lee, Seogwoo Hong, Jong-hyeon Chang
Seung Tae Choi (Univ. of Ulsan)

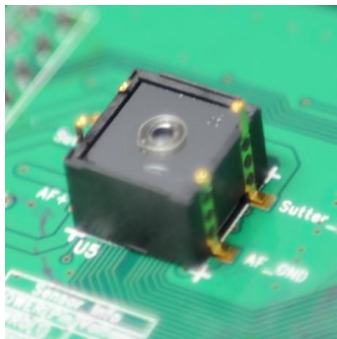
- MEMS AF module and global shutter are promising solutions for premium phone camera module in the future.
 - Slim, low cost and small size

Conventional Camera

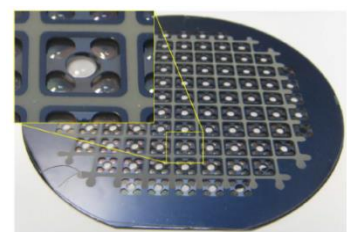
MEMS Camera



Parts-level fabrication and assembly



Wafer-level fabrication and assembly



MEMS Auto-Focus



(b) Single actuator with the spacer

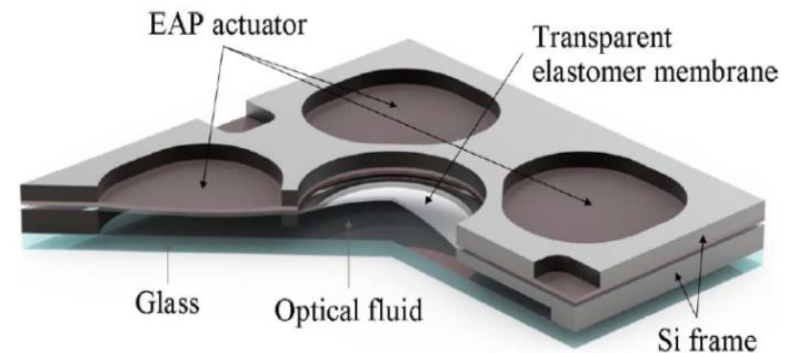
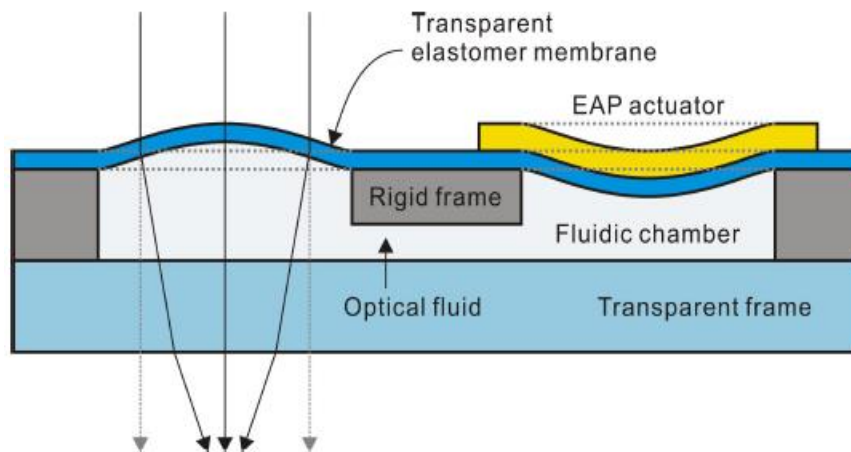
MEMS Global Shutter



Wafer-level Lens

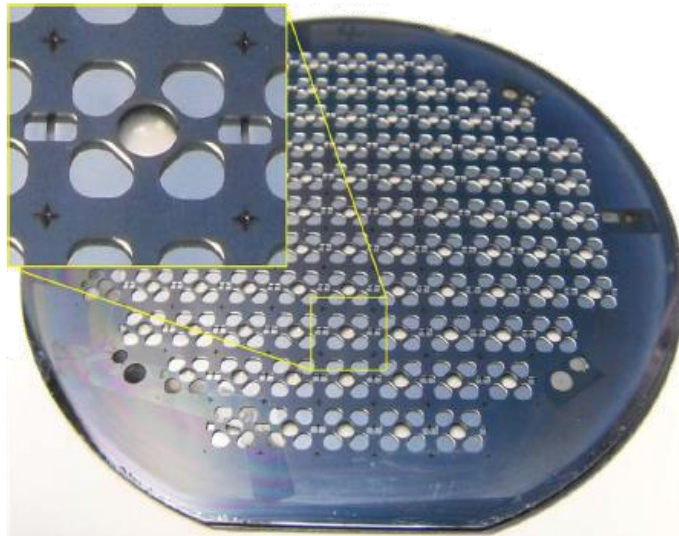
● EAP (electro-active polymer) actuated liquid lens for auto-focus

- Slim ($< 1\text{mm}$), Non-moving mechanism (noise-free)
- Lens surrounded by 4 chambers actuated by EAP
- Lens aperture, 2.4mm, and the device size was 7mm x 7mm x 0.9mm
- Add-on type AF lens for conventional camera modules

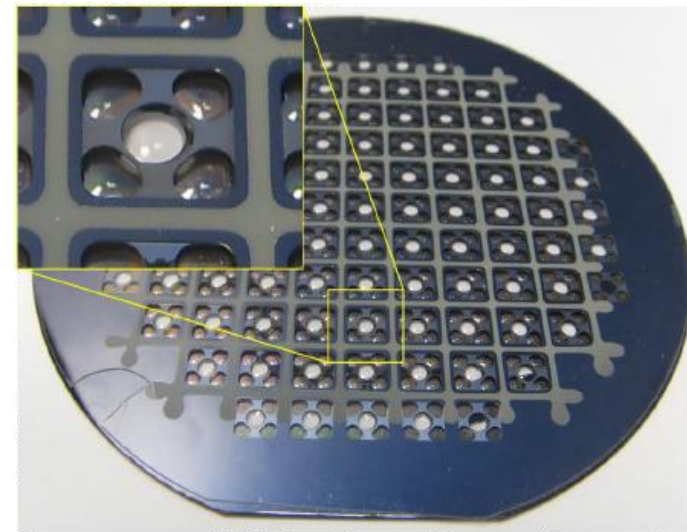


- **Liquid lenses are fabricated and assembled on 4 inch wafer with a glass substrate and two silicon wafers**
 - Micromachined and stacked with 4 inch wafers
 - 1 silicon wafer with chamber and channel structure
 - 1 glass wafer for bottom frame

Top-side View

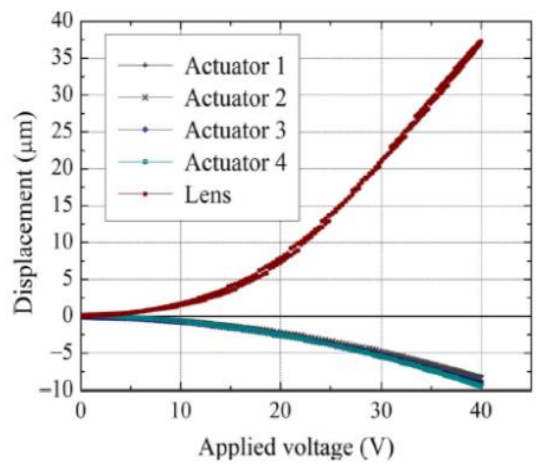


Bottom-side View

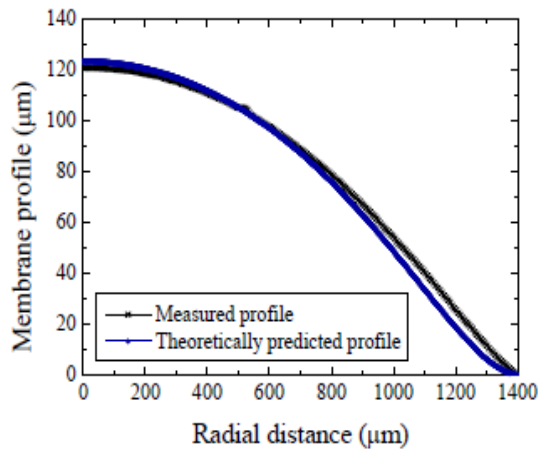


- **Lens profile is well controlled with applied voltage.**
 - Lens center displacement: 37 μm @ 40 volts
 - Profile was paraboloid showing quite good agreement with simulation
 - Good response for 50 Hz driving signals

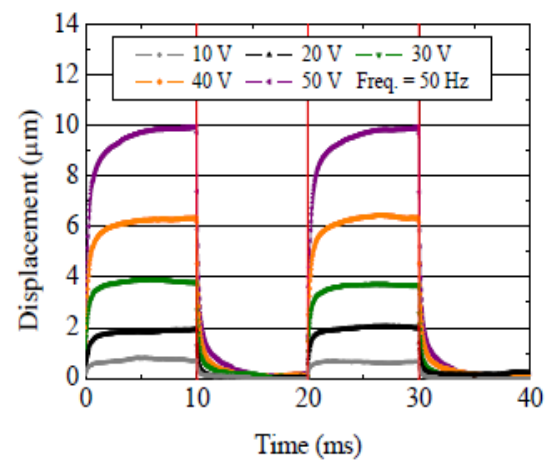
Voltage-dependent Responses



Deflected Displacement Profile



Time-dependent Responses



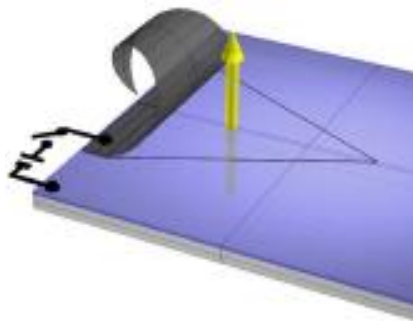
- A novel MEMS global shutter with small thickness ($\leq 1\mu\text{m}$) is proposed

- Concepts Design

- Precise control of residual stress of thin composite layers
- Electrostatic pull-in actuation

- Key features

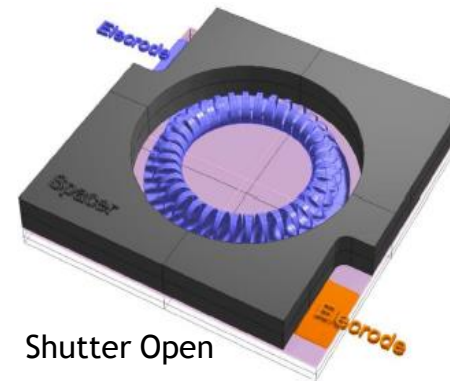
- Aperture size, 2.2mm
- 36 triangular roll actuators (leaf type)



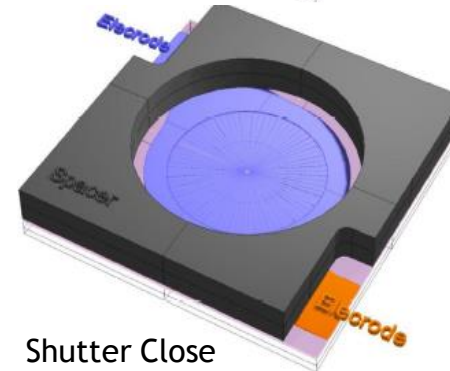
Leaf Open without voltage



Leaf Pull-down with voltage

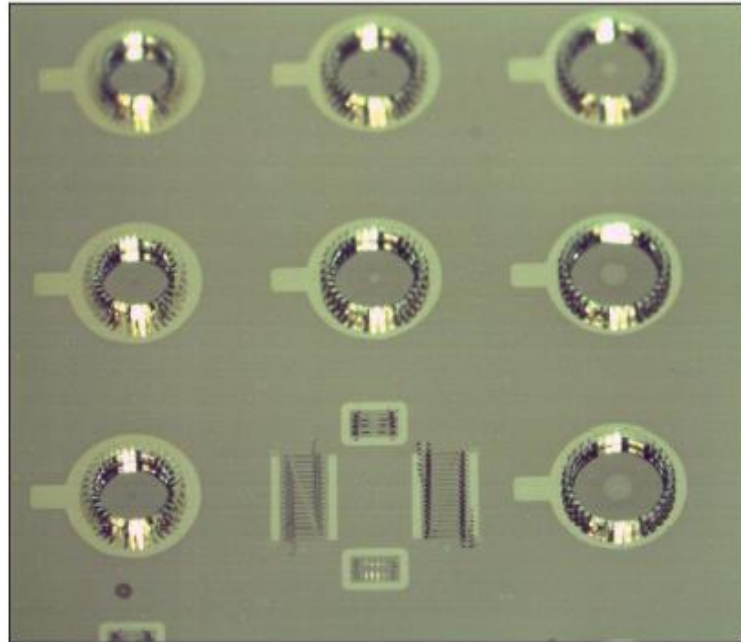


Shutter Open

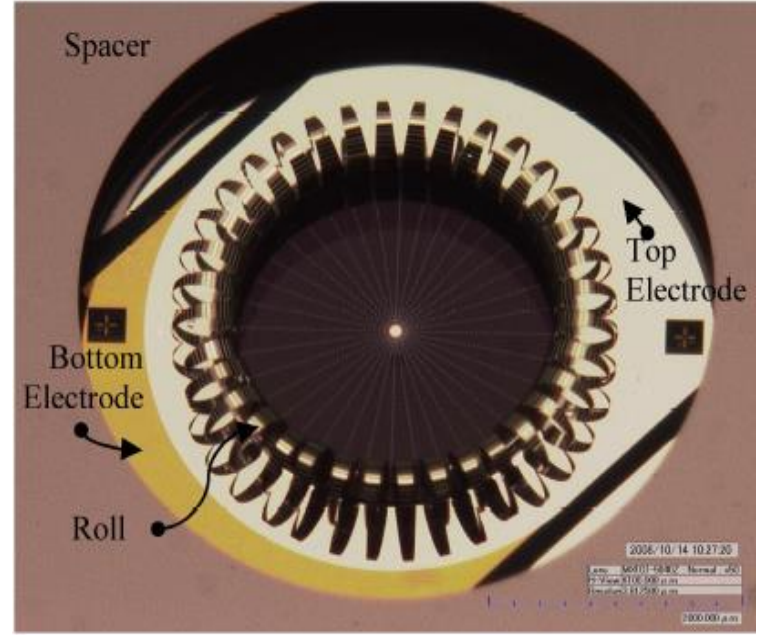


Shutter Close

- Shutter fabricated on 4 inch wafer
 - thickness of the shutter, 0.8mm
 - Radius of curvature, 225 μ m



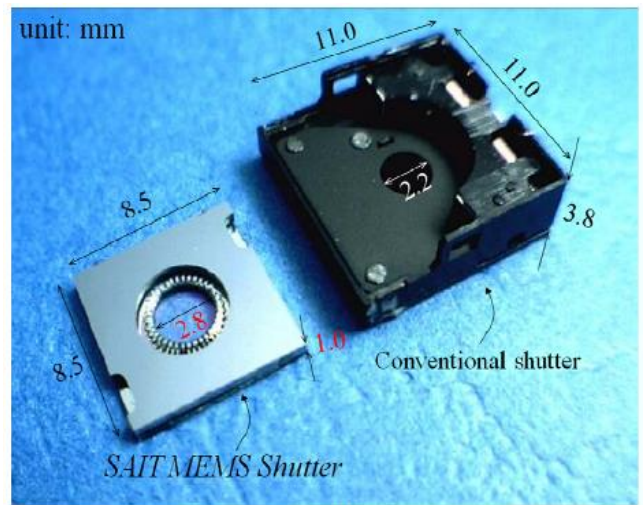
(a) Actuator only array on ITO glass



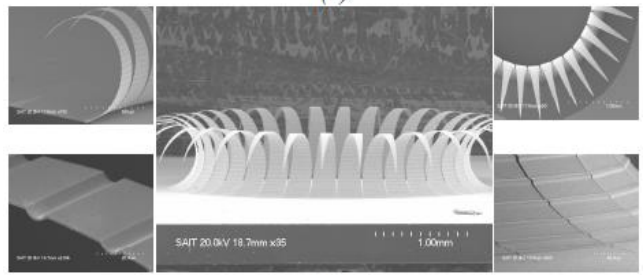
(b) Single actuator with the spacer

MEMS shutter is thinner with comparable performance

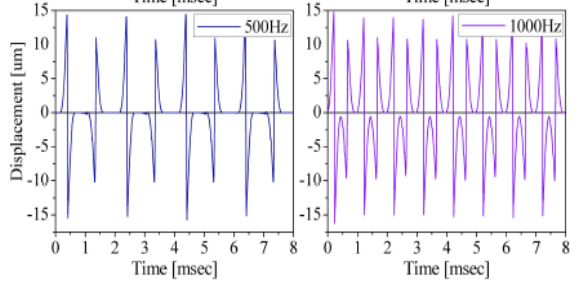
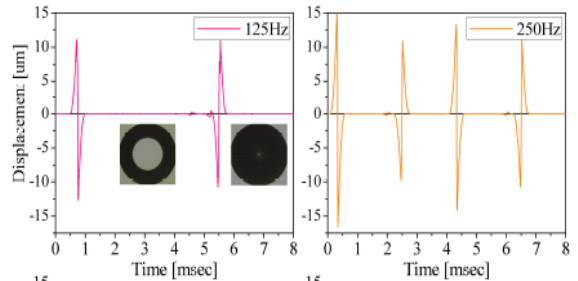
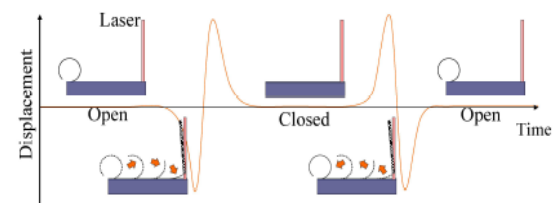
- Module thickness is 1mm (vs. 3.8mm of conventional one)
- Shuttering speed is 1/500sec actuated with 30V



(a)



(b)



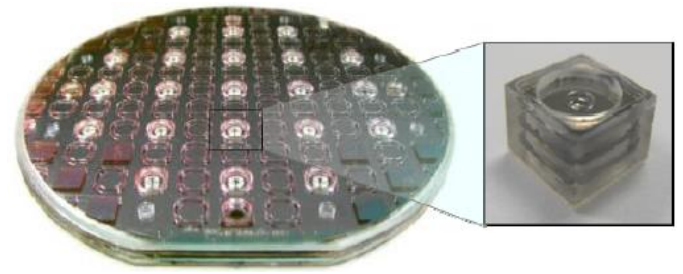
● Integration of shutter, auto-focus and lens module to complete the MEMS Camera assembly



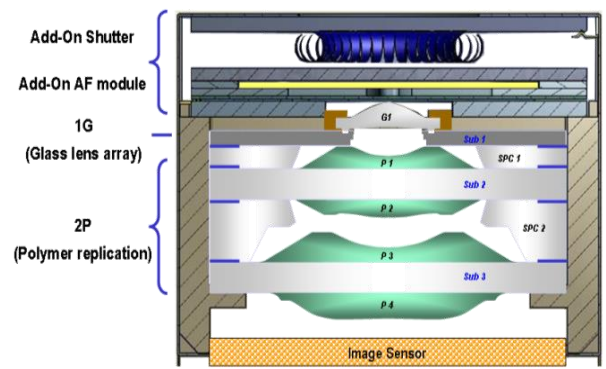
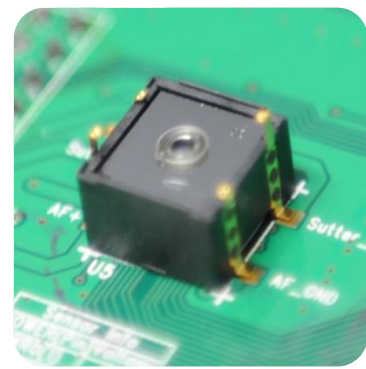
Shutter module



Auto Focus module



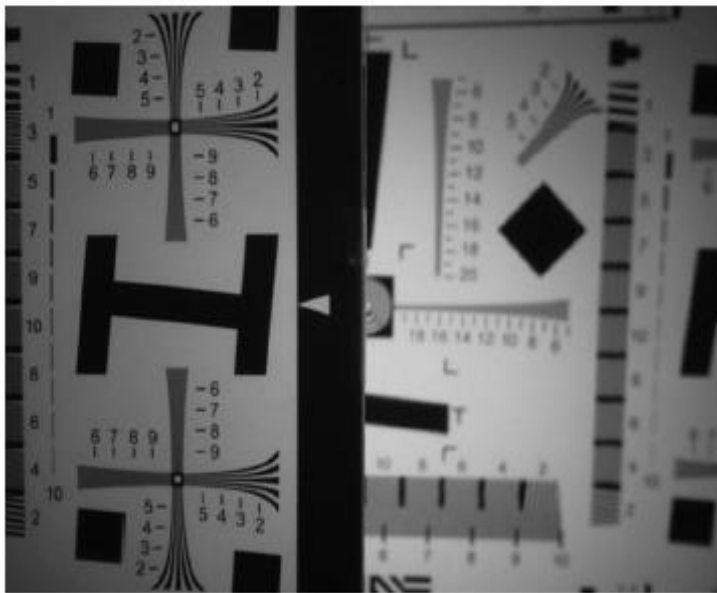
Lens module



MEMS Camera Assembly

- Our MEMS camera module shows comparable performance with a commercial phone camera module with 5 Mega pixels.
 - Auto-focus test for the images at 10cm and 120cm
 - MTF* is more than 30% at 180 lp/mm

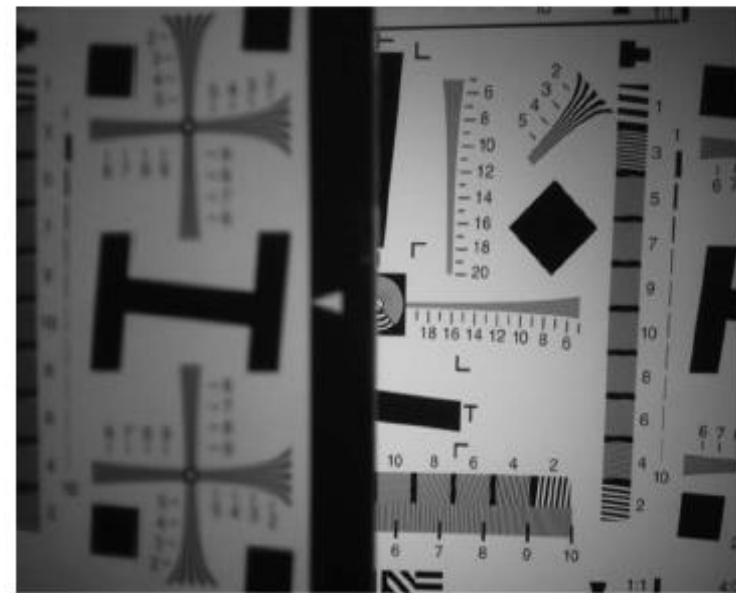
Focused at near object , left-hand side



Object @10cm

Object @120cm

Focused at far object, right-hand side



Object @10cm

Object @120cm

- Optical MEMS devices such as auto focus and global shutter were developed.
- These MEMS components as well as lens units were integrated to complete the camera module, and tested for performance

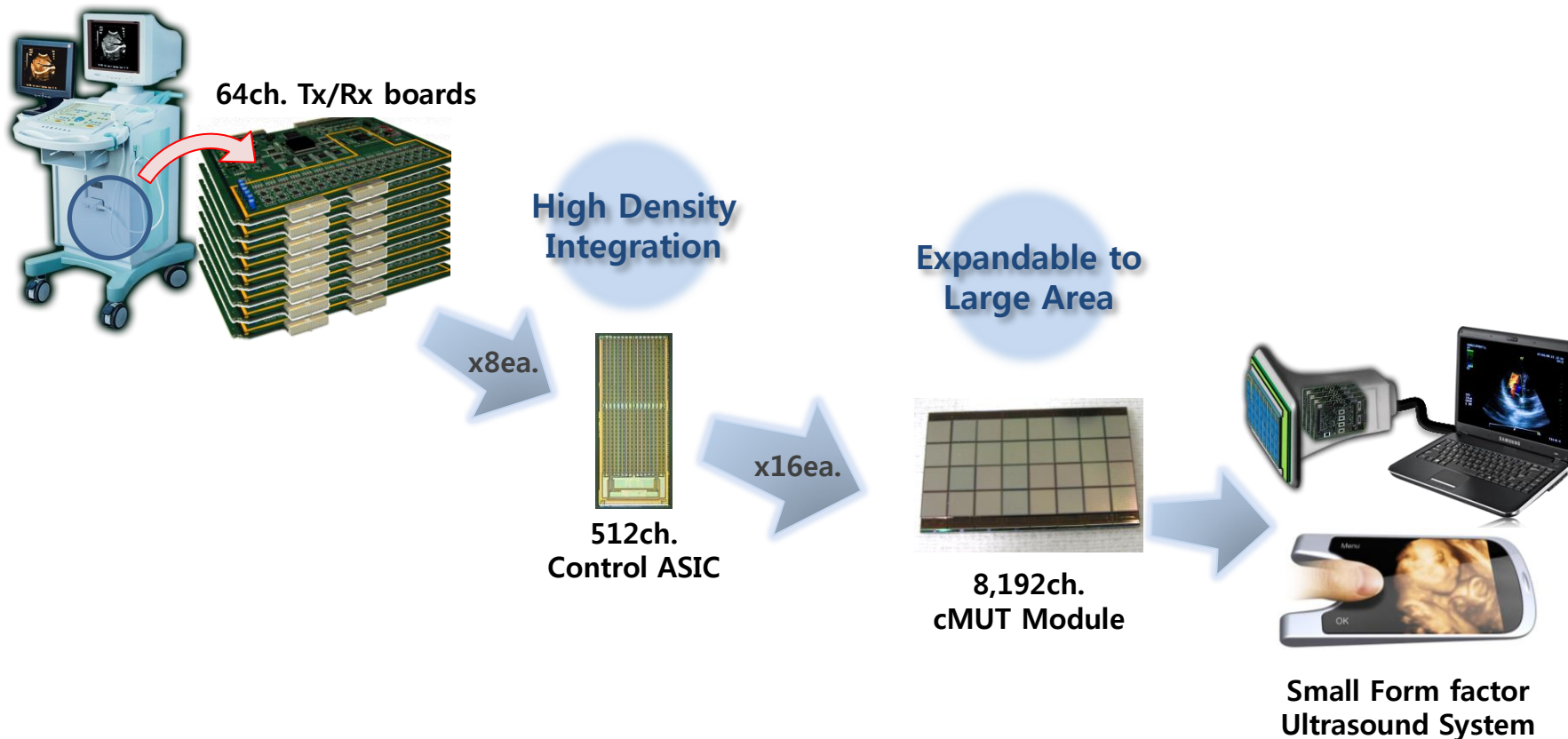
Acoustic MEMS

Ultrasonic Transducer with Improved Output



Contributors : Hyungjae Shin, Dong-Kyun Kim, Byung-Gil Jeong,
Seogwoo Hong, Seok-Whan Chung, and U-in Chung

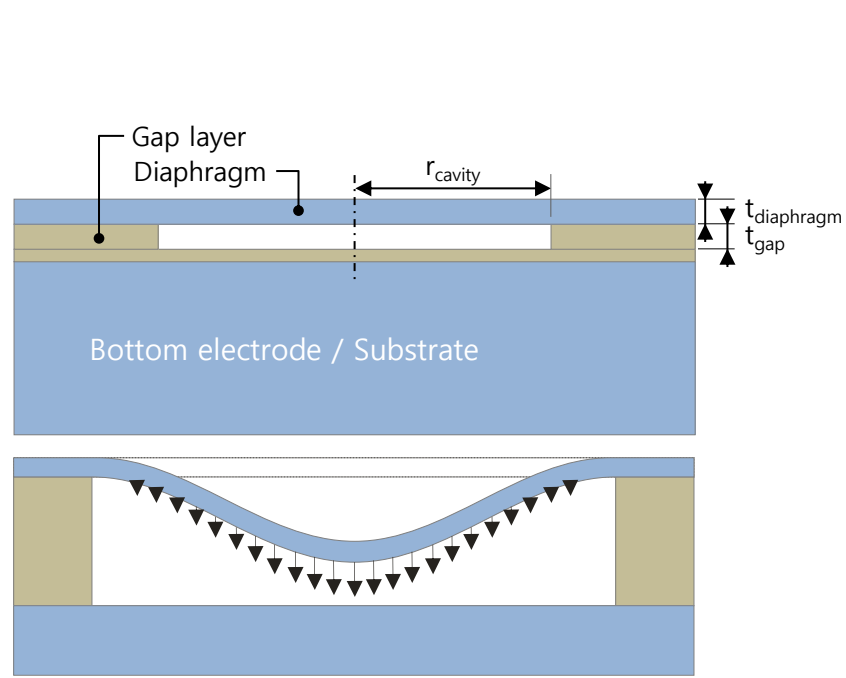
- Replacing machining-based current transducer with MEMS technology causes
 - Acquiring better performing transducer
 - High degree integration with control circuit leads to smaller form factor
 - Tiling methodology yields to expandable and flexible formats





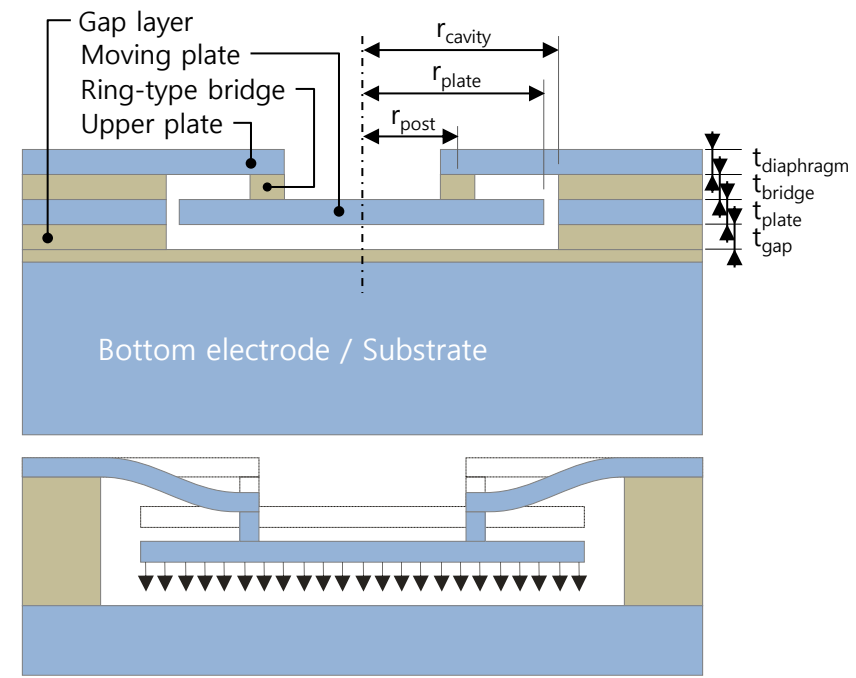
Conventional Basic Model

- Simplest form for high yield
- Radially varying force field as well as deflected volume



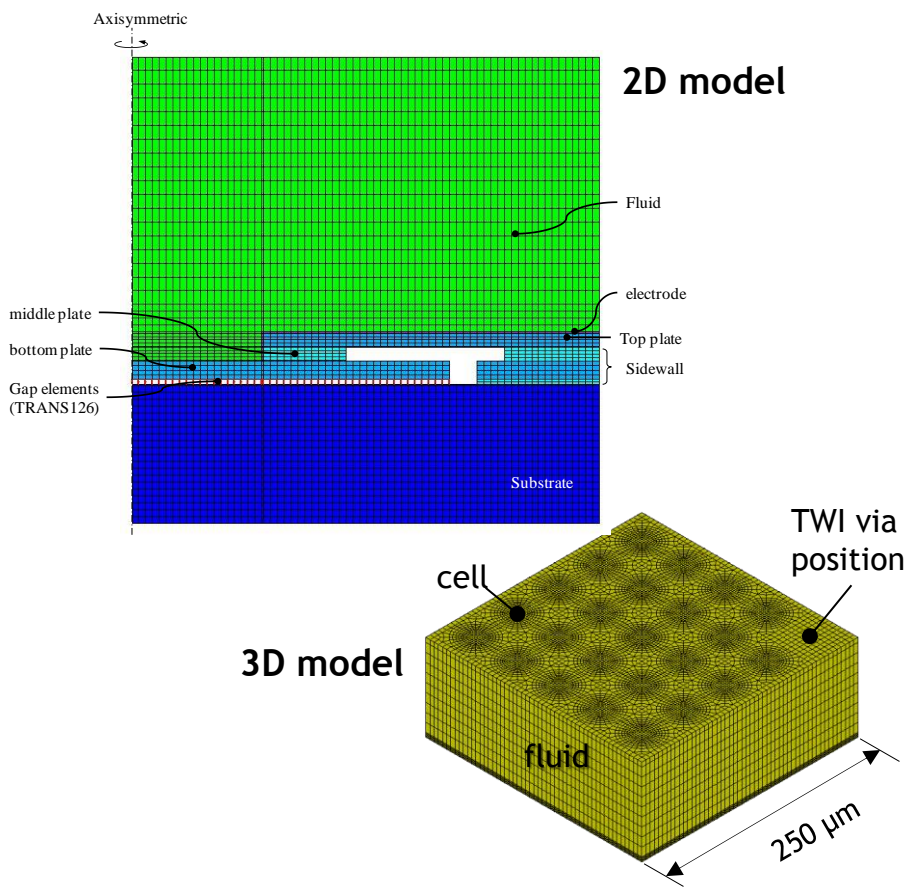
Indirectly Clamped Diaphragm Model

- Added element to divide roles
- Radially uniform force field as well as deflected volume



Simulation platform

- ANSYS program was used for calculation
- 2-dimensional model was created for fast screening of various combinations
- 3-dimensional model was adopted for more accurate estimations

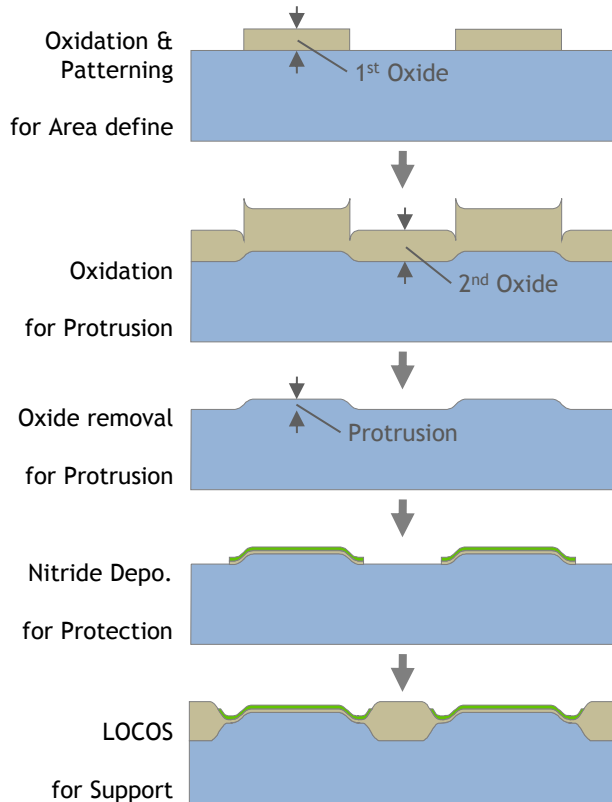


Dimensional Parameters	Conventional basic model [μm]	Indirectly clamped diaphragm model [μm]
element size	250	250
r_{cavity}	21	27
r_{plate}	-	23
r_{post}	-	12
t_{plate}	-	1
t_{bridge}	-	1.1
$t_{diaphragm}$	1	1.5
t_{gap}	0.4	0.35

• Device formation

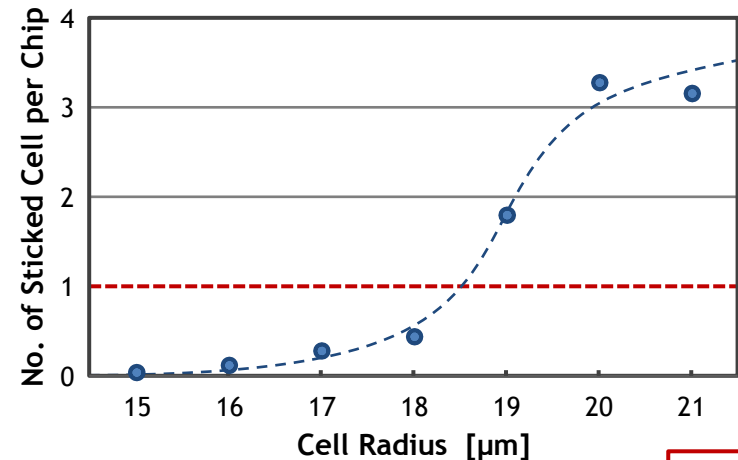
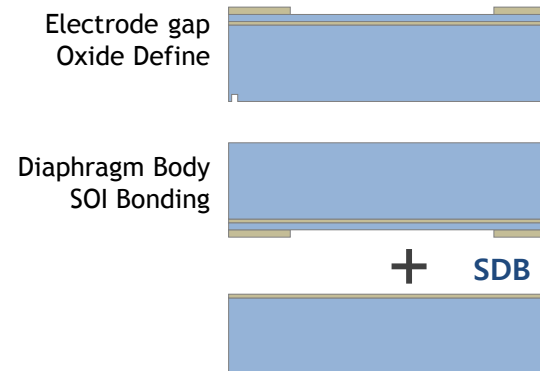
- LOCOS process : multi-step process with good resistance against charge accumulation
- Simple oxidation process : simple process, charge accumulation needs to be handled

LOCOS process



Stanford U., J. MEMS, 20.1.2011

Simple oxidation process

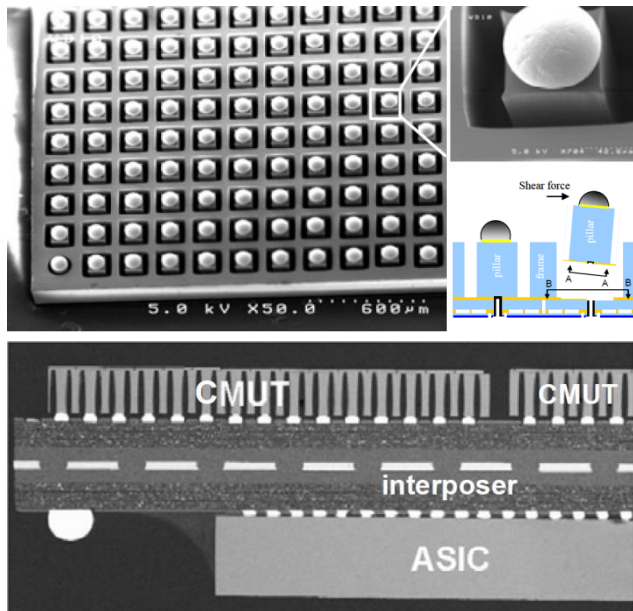


● Through-via Interconnect

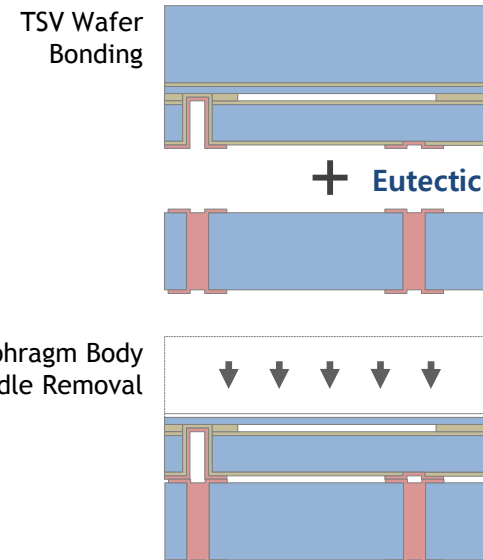
- Device fabricated with oxidation & wafer bonding process poses challenge for through via formation with its oxide layer in the middle

● Issues with DRIE and undercut at the oxide interface

- Limiting the feature size
- Mechanical instability
- Electrical connection failure



Stanford U., IEEE MEMS Conference, 2010

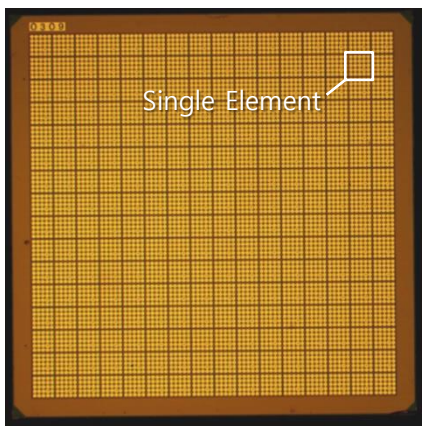


This work's approach

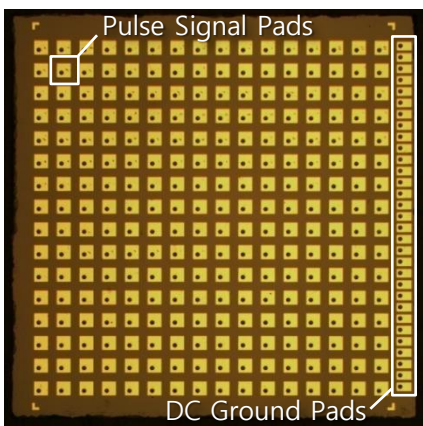
● Chip formation

- Single chip is consisted with 256 elements (16x16) and is designed to flip chip bonded to control ASIC, then tiled to form probe module of 8,192 elements (128x64)

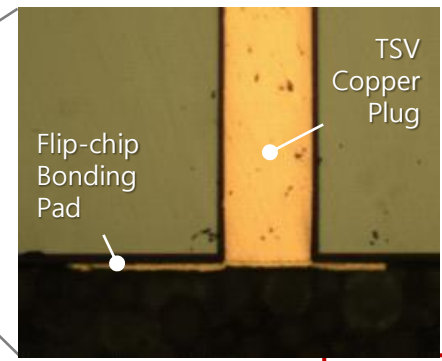
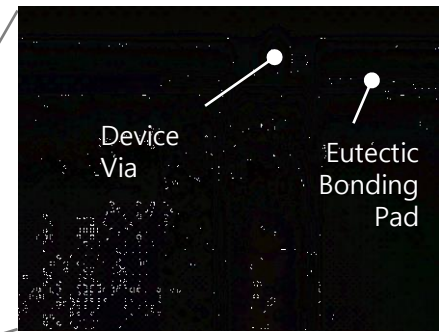
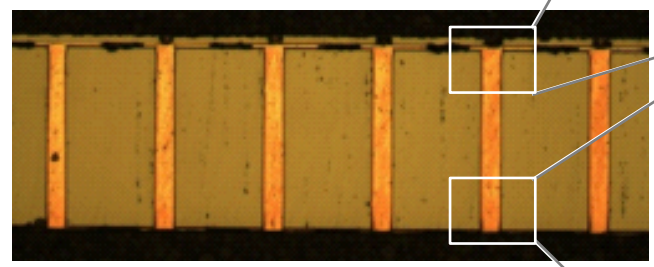
Top side



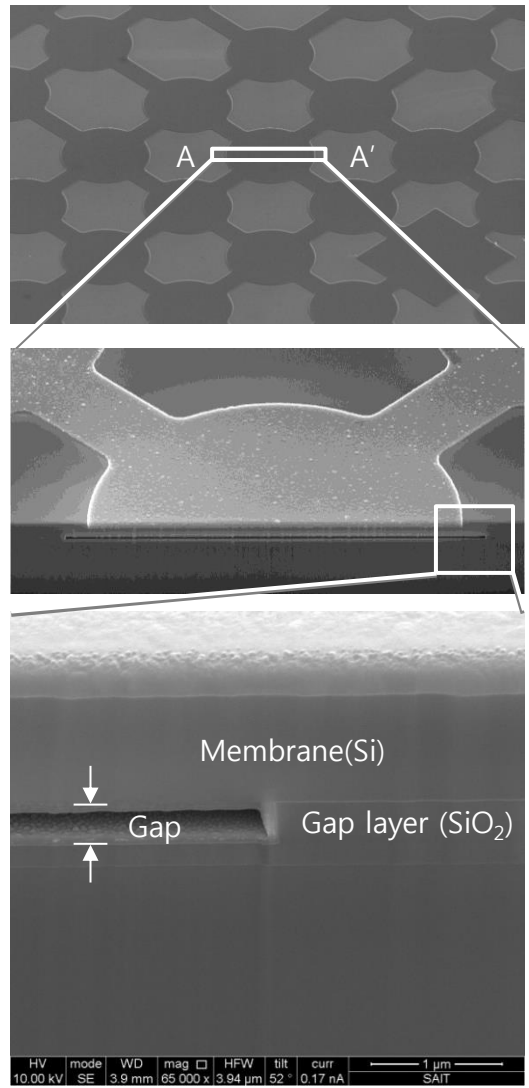
Bottom side



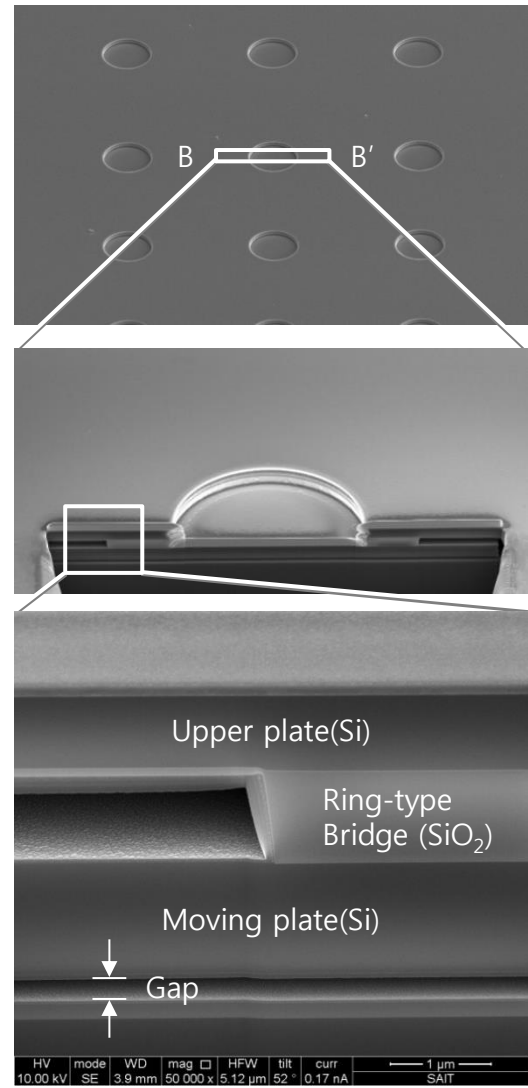
Cross section



Conventional Basic Model



Indirectly Clamped Diaphragm Model



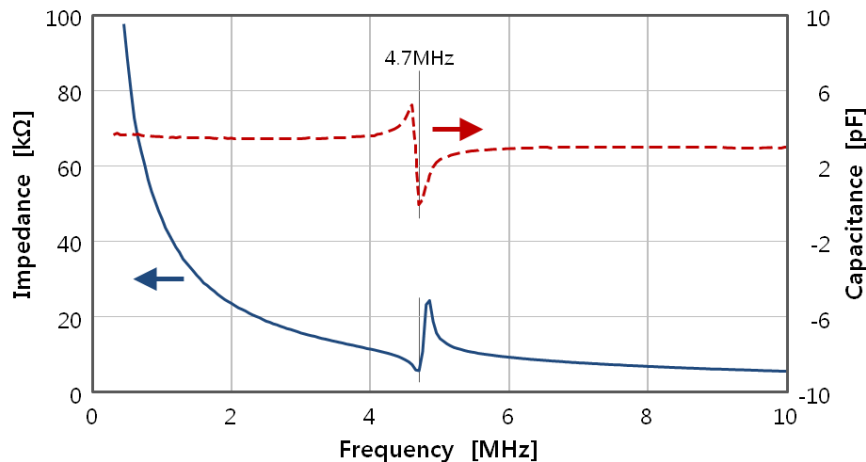
Electrical Properties

- Impedance : $> 20\text{k}\Omega$ at 2MHz with 90V_{DC} bias
- Capacitance : $3\sim 4\text{pF}$ except for resonant peak at 4.7MHz with 90V_{DC} bias

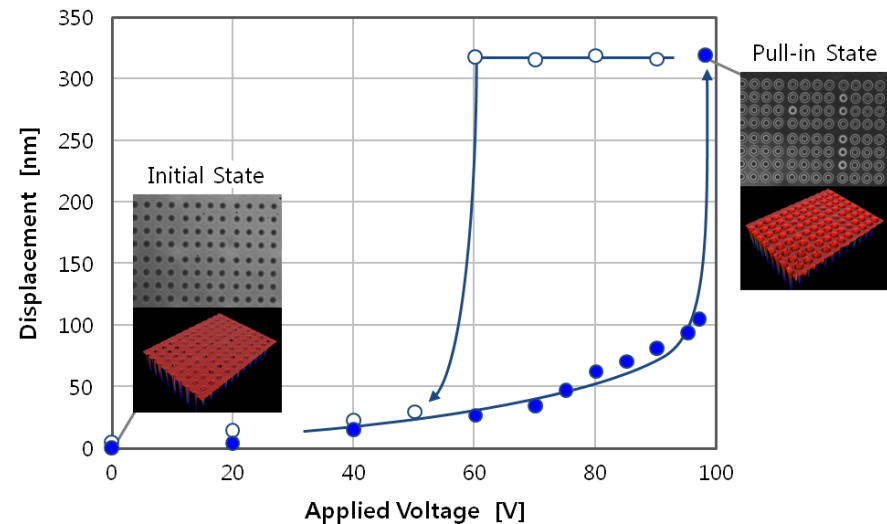
Pull-in Behavior

- Pull-in occurred at applied voltage of $97\sim 99\text{V}$ at $1/3$ of total displacement

Impedance & Capacitance



Displacement over Voltage



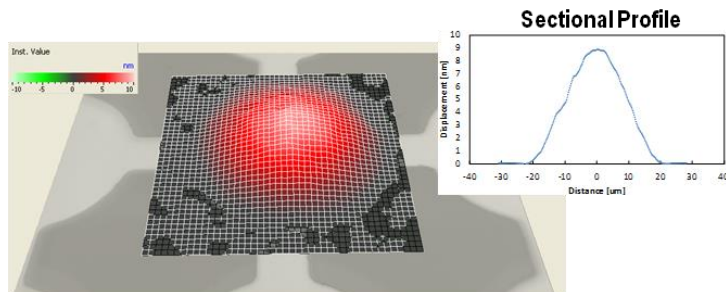
● Displacement Profiles

- Biased for 70% of pull-in voltage and excited with unipolar pulse of 20V
- Indirectly clamped diaphragm model exhibits flatter displacement configuration which is closer to the piston motion

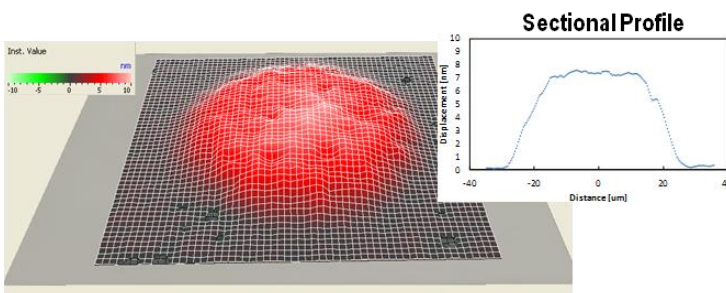
● Resonant Frequencies

- Two models exhibited different resonant frequencies in air condition
- Resonant frequencies for two models in oil were same at ~3.5MHz as designed

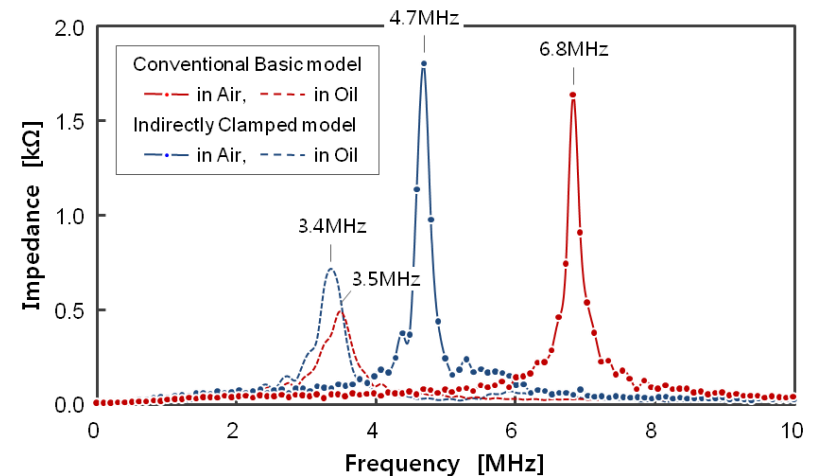
Conventional Basic Model



Indirectly Clamped Diaphragm Model

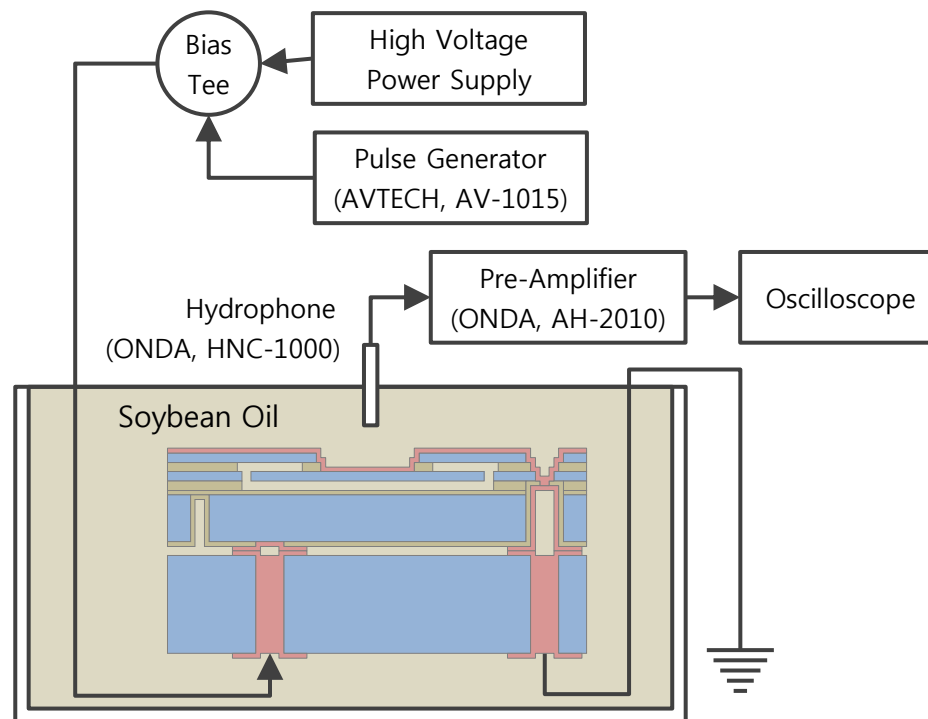


Resonance Characteristics in Air



Measurement Setup and Conditions

- Measurement in transmission mode
- Bias voltage : 81V for basic model and 67V for indirectly clamped model
- Pulse voltage : unipolar pulse train of 20 V_{pp} & 40 nsec duration, 125μsec period
- Hydrophone, HNC-1000, ONDA corp., was positioned at 5mm from the surface
- Captured acoustic signal was amplified, AH-2010, ONDA corp., with 20 dB gain



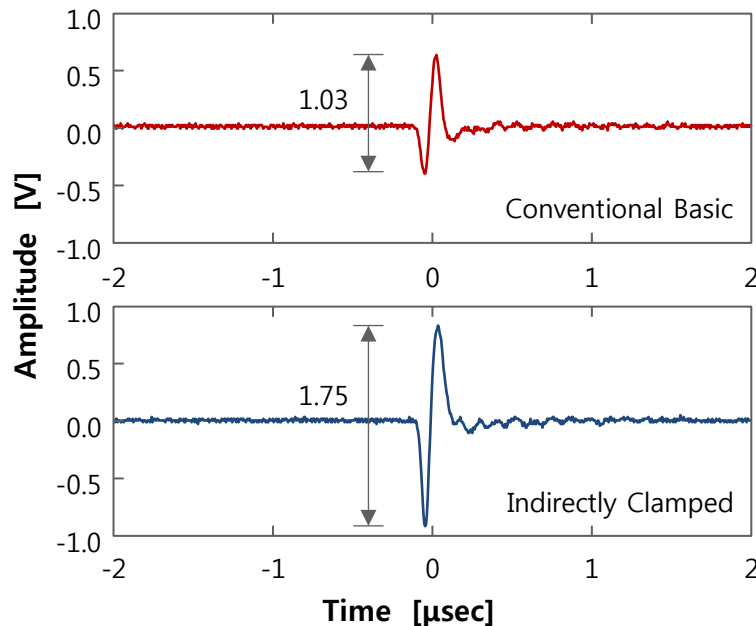
● Output pressure

- 1.7 times more peak-to-peak acoustic amplitude for indirectly clamped diaphragm model over conventional basic model

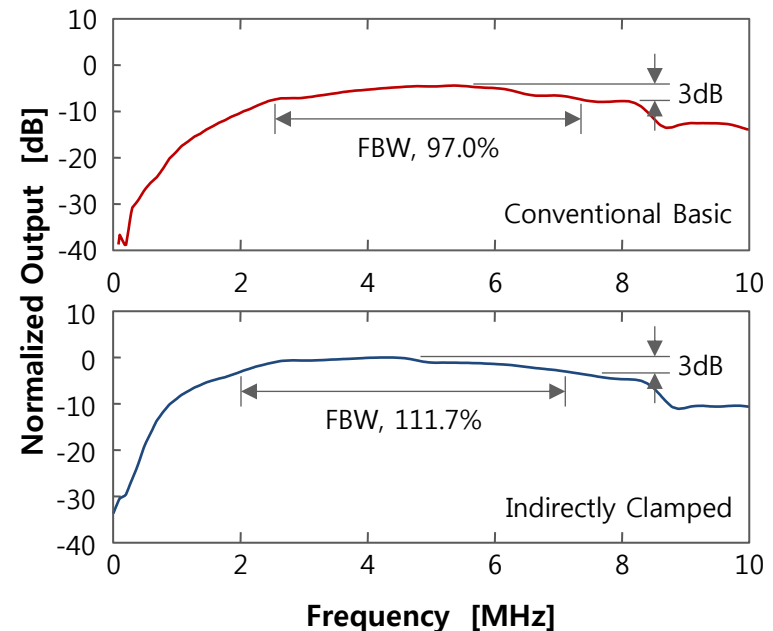
● Fractional Bandwidth

- Indirectly clamped diaphragm exhibits 14.7% more fractional bandwidth than the basic model

Output Pressures

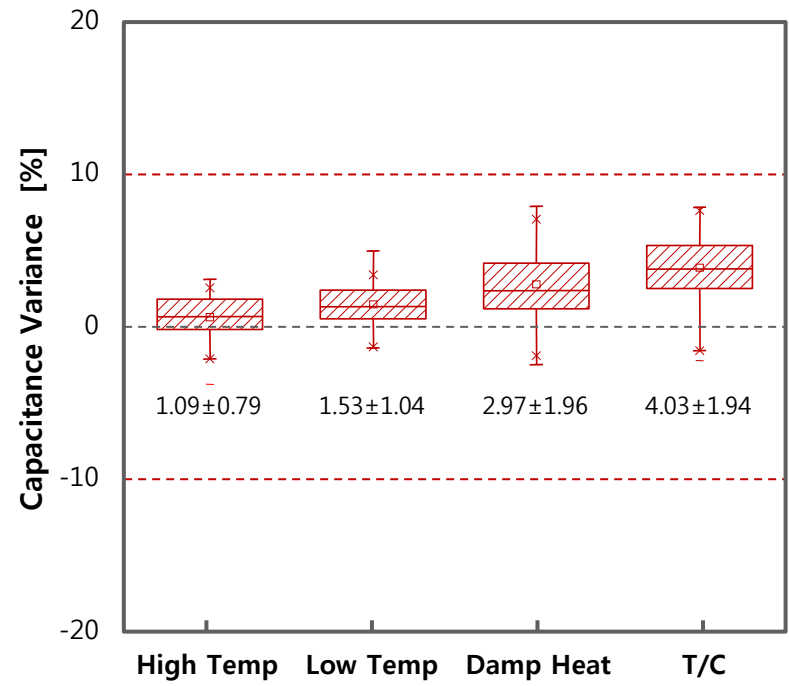
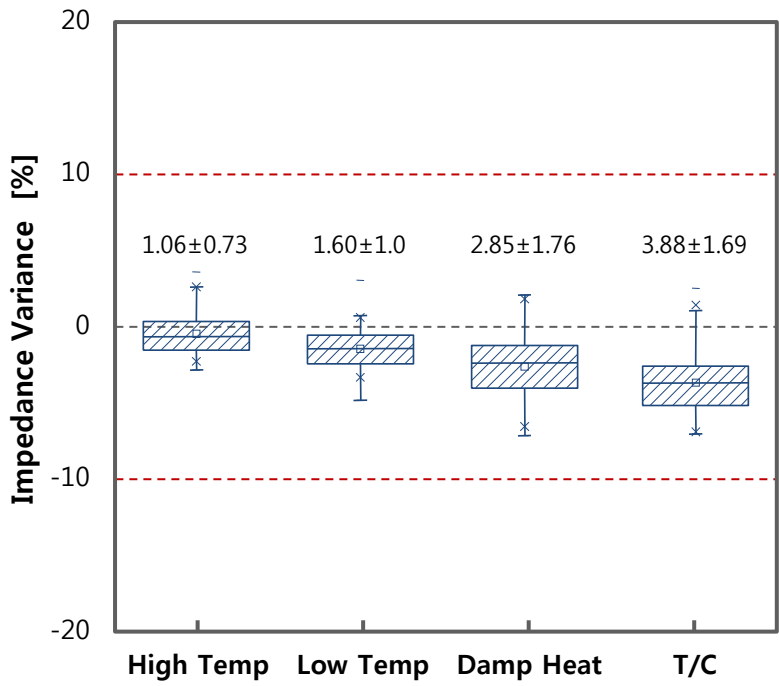


Frequency Responses



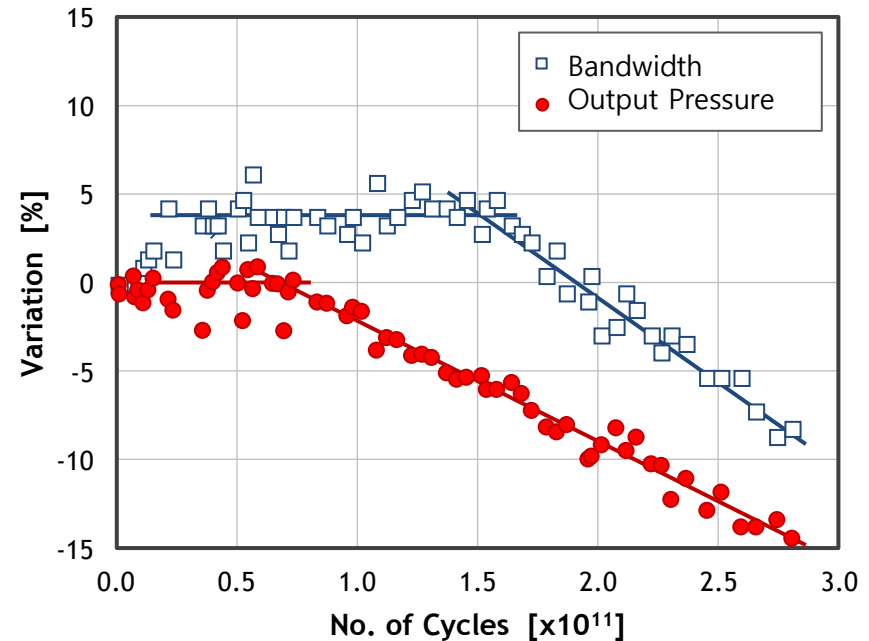
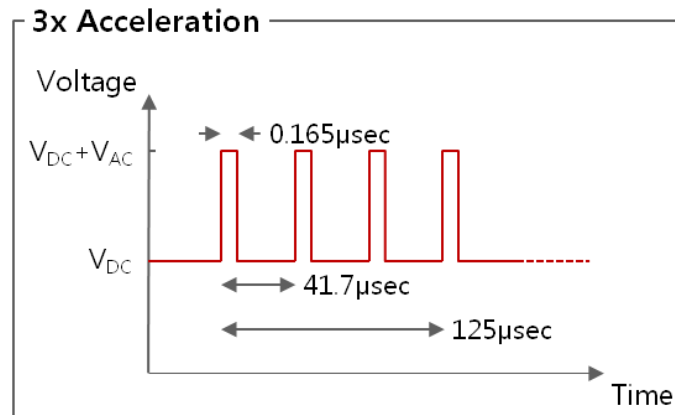
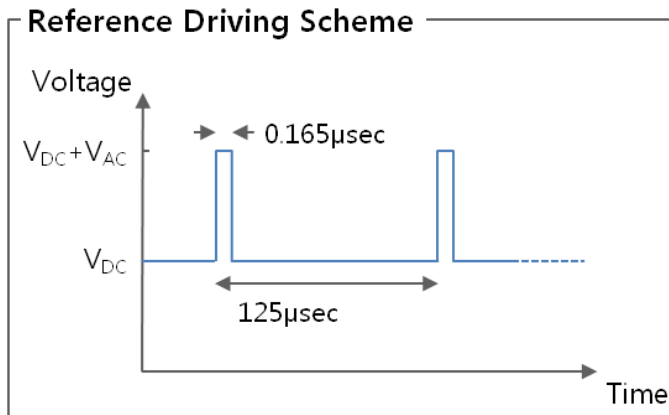
Evaluation, Environmental Reliability

Environmental Storage Tests	Test Conditions	Pass/Fail Guideline	Sample Size	Reference
High temperature	+85°C for 96hrs.	Performance parameters - Input Impedance - Capacitance	20 ea.	JEDEC22-A103C (Condition G)
Low temperature	-40°C for 96hrs.			RS C 0149 (intensified)
Damp heat	+85°C & 85%RH for 96hrs.	JEDEC22-A101B		
Temperature cycling	-55°C ~ +85°C for 200cycles with 15min. dwell	Performance Variation - less than ±10%		JEDEC22-A104B (Condition A)



Measurement conditions

- 8x8 TEG sample 5ea. after burn-in of 96hrs. at 85°C & 85%RH
- Driving : $50V_{DC} + 50V_{Pulse}$ with 165nsec pulse at 3x accelerated speed
- Environment : immersed in vegetable Oil at 40°C
- Measurement : output pressure & bandwidth measured at 5mm from cMUT surface



● Lifetime Calculation

- 60 element TEG result needs to be correlated to 8,192 element probe module
- Target lifetime of 0.8×10^6 sec for TEG translated to probability of 2.1×10^{-6} , then converted to probe module's 2.9×10^{-4} and lifetime of 8.16×10^6 sec
- From the measurement, initial failure occurred at 22.23×10^6 sec, therefore, lifetime to be estimated as 2.7 times longer than required value with 95% confidence level.

$$F(t) = \int_0^t f(t) \cdot dt$$

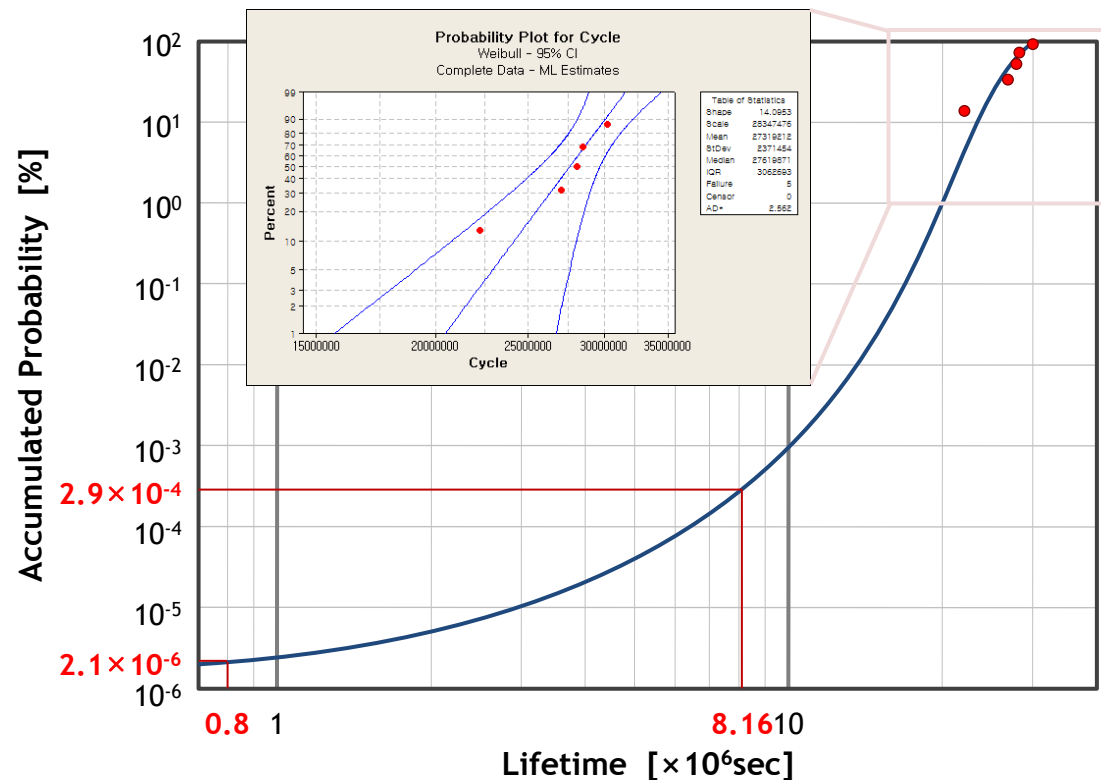
$$F_M = 1 - \left\{ {}_{137}C_0 \cdot F_T^0 \times (1 - F_T)^{137} \right\}$$

$f(t)$: probability for failure

$F(t)$: accumulated probability for failure

F_M : accumulated probability of module

F_T : accumulated probability of TEG



- **New concept of cMUT was disclosed**

- 70% more output pressure and 15% more bandwidth were observed with comparable resources
- Integration with control ASIC was made possible with through-via interconnection
- Environmental reliability was confirmed, and lifetime was estimated to be 2.7 times to the required value.